JOURNAL OF Materials CHEMISTRY

Thermal decomposition of Mg/Al and Mg/Ga layered-double hydroxides: a spectroscopic study

María A. Aramendía, Yolanda Avilés, Victoriano Borau, José M. Luque, José M. Marinas, José R. Ruiz* and Francisco J. Urbano

Dpto. Química Orgánica, Avda. San Alberto Magno s/n, Universidad de Córdoba, 14004 Córdoba, Spain

Received 20th January 1999, Accepted 15th April 1999

An Mg/Al and a Mg/Ga layered double hydroxide (LDH) were synthesized by using the coprecipitation method and calcined at a variety of temperatures. The starting LDHs and their calcination products (mixtures of oxides and spinels) were characterized by X-ray diffraction, solid-state NMR and IR spectroscopies and thermogravimetric analysis. Based on the results, the LDHs studied possess a brucite-like structure where tervalent cations occupy octahedral positions. At moderate temperatures, calcination gives a mixture of oxides; at high temperatures, however, the corresponding spinels are obtained.

Introduction

Hydrotalcite, $[Mg_6Al_2(OH)_{16}](CO_3)\cdot 4H_2O$, is a layered-double hydroxide (LDH) belonging to the anionic clay family[1] structurally analogous to brucite, $Mg(OH)_2$; Mg^{2+} cations occupy the centres of octahedra, which are superimposed and joined by hydrogen bonds between hydroxy groups at octahedron vertices. In hydrotalcite some Mg^{2+} ions are replaced by Al^{3+}; this produces a charge deficiency in the layers that is neutralized by anions in the interlayer region, which also contains water of crystallization. Replacement of the magnesium or aluminium with another cation (Ni, Zn or Cu in the former case and Ga, Cr, Fe or Mn in the latter) yields the so-called layered-double hydroxides, of general formula $[M^{II}_{1-x}M^{III}_x(OH)_2]^{x+}(A^{n-})_{x/n}\cdot mH_2O$. These solids are currently being used in many catalysed processes including condensation,[2,3] hydrogenation[4,5] and nitrogen oxide decomposition reactions,[6,7] among others.

Characterizing surface active sites in catalysts is one of the primary goals in catalysis that has so far been pursued by using a wide variety of instrumental techniques such as XRD, IR, Raman, NMR, EPR and ESCA spectroscopies. Thus, multinuclear MAS NMR spectroscopy was recently used by our group for the structural elucidation of catalytically active solids such as sepiolites,[8] magnesium oxide–magnesium orthophosphate systems,[9] magnesium pyrophosphate[10] and silica–aluminium phosphate systems.[11]

The chemical nature of zeolites in catalytically active materials is altered by the isomorphic substitution of Al^{3+} by Ga^{3+}; this can be used with a view to designing improved zeolite catalysts and zeolite-based molecular sieves.[12–14]

The growing interest in the use of Ga^{3+} in catalytic systems led us to investigate an Mg/Ga layered double hydroxide (LDH) and compare it with an Mg/Al LDH that is widely documented in the literature. The study included both LDHs as such and their products upon calcination at a variety of temperatures, and involved the use of various instrumental techniques such as X-ray diffraction (XRD), diffuse reflectance IR (DRIFT) spectroscopy and magic-angle solid-state MAS NMR spectroscopy.

Experimental

Preparation of LDHs

Mg/Al LDH. Two solutions containing 0.03 mol of $Mg(NO_3)_2\cdot 6H_2O$ and 0.01 mol of $Al(NO_3)_3\cdot 6H_2O$, respectively, in 25 ml of deionized water, were mixed and the mixture added dropwise to 75 ml of an Na_2CO_3 solution at pH 10 at 333 K under vigorous stirring. The pH was kept constant by adding appropriate volumes of 1 M NaOH during precipitation. The suspension thus obtained was kept at 353 K for 24 h, after which the solid was filtered off and washed with 2 l of deionized water.

Mg/Ga LDH. The procedure used to prepare this compound was identical to that above except that the starting solutions contained 0.03 mol of $Mg(NO_3)_2\cdot 6H_2O$ and 0.01 mol of $Ga(NO_3)_3\cdot 6H_2O$.

Once synthesized, the LDHs were exchanged with carbonate in order to remove nitrate ions from the interlayers. For this purpose, 2.5 g of LDH was dispersed in 125 ml of distilled water and 250 mg of Na_2CO_3 was added and the mixture allowed to reflux for 2 h, after which the solid was separated by centrifugation and the water discarded. This operation was repeated and the supernatant analysed for nitrate, which gave a negative test. The resulting solids, denoted HT-Mg/Al and HT-Mg/Ga, were dried at 373 K and calcined in a nitrogen atmosphere at 473, 773, 1073 or 1273 K for 8 h.

Characterization

The elemental composition of the samples was determined on a Perkin-Elmer 1000 ICP spectrophotometer under standard conditions.

X-Ray diffraction (XRD) patterns were recorded on a Siemens D-500 diffractometer using Cu-Kα radiation. Scans were performed over the 2θ range from 5–80°.

Thermogravimetric curves were recorded on a Cahn 2000 electrobalance by heating from 298 to 1073 K at 10 K min^{-1} in an argon atmosphere.

FTIR spectra for the LDHs at room temperature and for samples calcined at 473 K, and diffuse reflectance IR (DRIFT) spectra for the calcined solids at different temperatures were recorded over the wavenumber range 400–4000 cm^{-1} on a Bomen MB-100 FTIR spectrophotometer. Samples were prepared by mixing the powdered solids with KBr (the blank) in a 15 : 85 ratio.

The specific surface areas of the solids were determined by the BET method[15] which was implemented on a Micromeritics ASAP 2000 analyser.

^{27}Al and ^{71}Ga MAS NMR spectra were recorded at 104.26 and 121.98 MHz, respectively, on a Bruker ACP-400 spectrometer under an external magnetic field of 9.4 T. All measure-

ments were made at room temperature. The samples, held in zirconia rotors, were spun at the magic angle (54° 44′ relative to the external magnetic field) at 3.5 kHz for ^{27}Al and 5.0 kHz for ^{71}Ga. ^{27}Al spectra were recorded at an excitation pulse of $\pi/8$ (0.6 μs) and an accumulation interval of 1 s. ^{71}Ga spectra were obtained at an excitation pulse of $\pi/4$ (2 μs) and an accumulation interval of 1 s. $Al(H_2O)_6^{3+}$ and $Ga(H_2O)_6^{3+}$ were used as external standards for aluminium and gallium, respectively.[16] The number of accumulations for ^{27}Al and ^{71}Ga spectra were 1000 and 60 000, respectively.

Results and discussion

Elemental analysis

Elemental analysis of the LDHs following ion exchange with carbonate and drying at 393 K provided the following ratios: 3:1 Mg:Al in HT-Mg/Al and 3:0.84 Mg:Ga in HT-Mg/Ga. The resulting formulae for the LDHs can thus be written as $Mg_{0.75}Al_{0.25}(OH)_2(CO_3)_{0.125}\cdot 0.70H_2O$ and $Mg_{0.78}Al_{0.22}(OH)_2(CO_3)_{0.120}\cdot 0.62H_2O$, respectively.

XRD results

The XRD patterns for the LDHs (Figs. 1A and 2A) exhibit some common features of layered materials (*e.g.* narrow, symmetric, strong lines at low 2θ values and weaker, less symmetric lines at high 2θ values). A comparison of the XRD patterns for the sample containing gallium with that for the aluminium sample reveals that the former possess the same layered structure as the Mg/Al hydrotalcite. From the position of the strongest lines, of crystallographic indices (003) the lattice distance, d_{003}, was calculated and used to determine the lattice parameter c (23.16 and 23.39 Å for HT-Mg/Al and HT-Mg/Ga, respectively). These values suggest that the insertion of Ga^{3+}, a larger cation than Al^{3+}, in the LDH structure increases the spacing between layers. Structural changes produced by calcination of the LDHs samples at 473 K (Fig. 1B and 2B) caused no alteration or any significant change in the structures. On the other hand, a calcination temperature of 773 K destroyed the LDH structure and led to the formation of a periclase MgO phase in addition to amorphous aluminium or gallium oxides (Fig. 1C and 2C). These results are consistent with previous findings that periclase MgO is the sole crystalline phase expected to occur at these calcination teperatures.[17] Raising the calcination temperature to 1073 K resulted in no change in the phases obtained except for increased crystallinity in the samples. Finally, raising the temperature from 1073 to 1273 results in a sharpening of the MgO reflections. At this temperature, sharp reflections for spinel ($MgAl_2O_4$ and $MgGa_2O_4$) also appear (Fig. 1E and 2E, respectively).

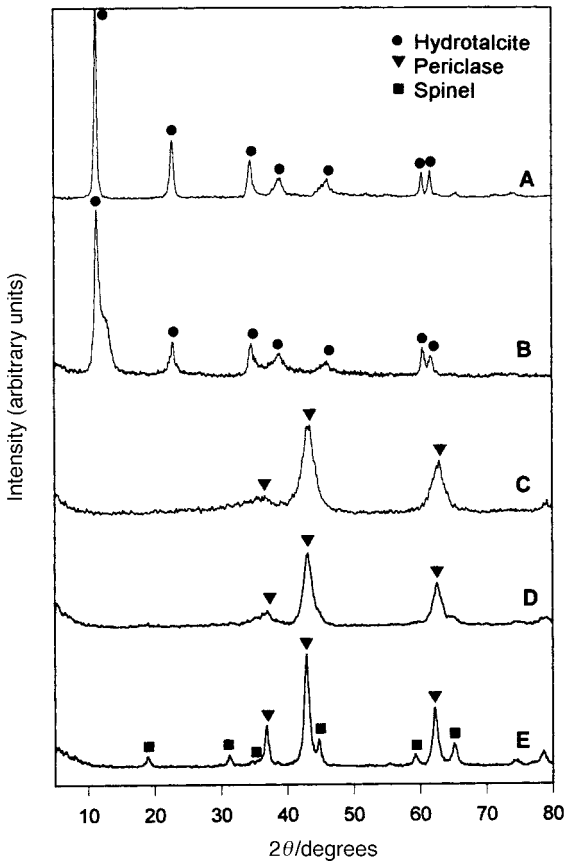

Fig. 1 XRD patterns for HT-Mg/Al (A) and its products of calcination at 473 K (B), 773 K (C), 1073 K (D) and 1273 K (E).

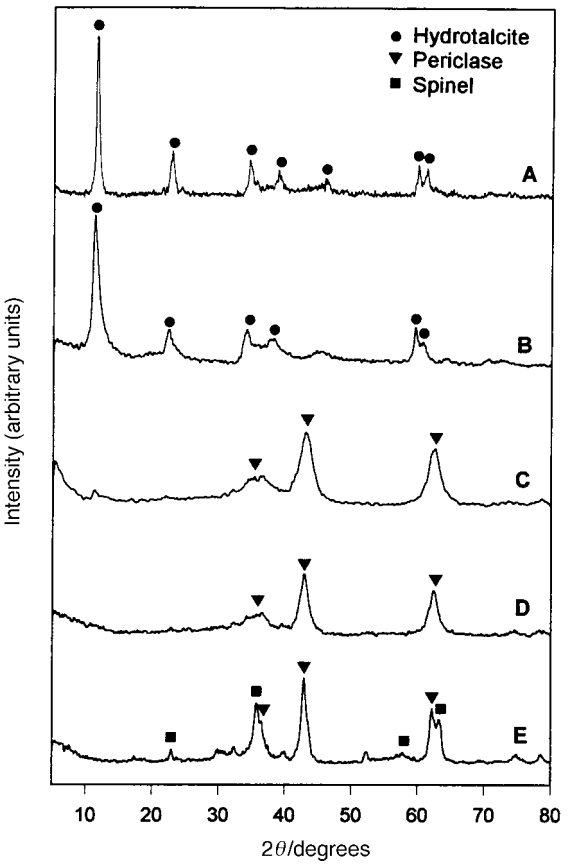

Fig. 2 XRD patterns for the HT-Mg/Ga (A) and its products of calcination at 473 K (B), 773 K (C), 1073 K (D) and 1273 K (E).

TGA results

The TGA curves for the two samples (Fig. 3) exhibit three main regions over the temperature ranges 300–540, 540–800 and 800–1073 K, which involve an overall weight loss of 44.8% for HT-Mg/Al and 39.7% for HT-Mg/Ga. The first such loss (15.9 and 13.1% for HT-Mg/Al and HT-Mg/Ga, respectively) can be attributed to the release of interparticle pore water;[18] the second weight loss (28.9% for HT-Mg/Al and 26.6% for HT-Mg/Ga) is due to the removal of carbonate ions from the interlayer and hydroxide ions from the brucite-like layer.[18,19] Over this temperature range, the LDHs undergo decarbonation and dehydroxylation reactions that release carbon dioxide and water, and produce metal oxides. The third, final weight loss, of lesser significance than the previous two, involves the sustained release of water above 800 K. This water probably results from dehydroxylation of the Al_2O_3 or Ga_2O_3 phase. This third weight loss is somewhat controversial. Based on mass spectra obtained during the thermal decomposition of

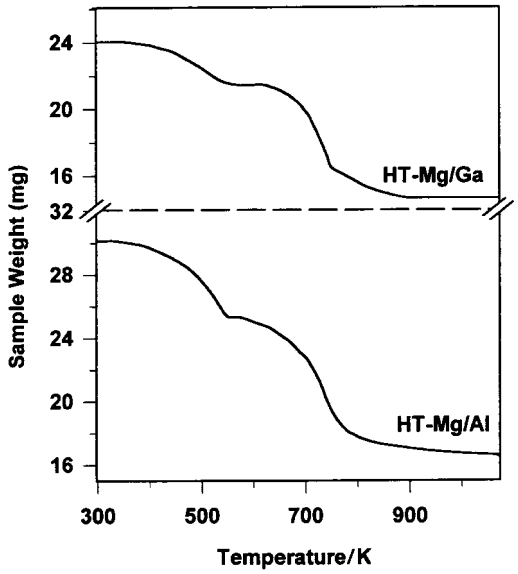

Fig. 3 TGA curves for the LDHs.

LDHs, some authors have ascribed it to loss of water;[20] others, however, have related it to removal of carbonate ions.[21,22]

MAS NMR spectra

Fig. 4 shows the ^{27}Al MAS NMR for solid HT-Mg/Al and its calcination products. The observed chemical shifts exclude the requirement for second-order quadrupole correction. As can be seen from Fig. 4A, the spectrum for the uncalcined LDH contains a single signal at δ 9.7. This suggests that aluminium occupies octahedral sites (Al_O) preferentially. The loss of interlayer water at 473 K gives a small resonance at δ 74 (Fig. 4B) that can be assigned to tetrahedrally coordinated aluminium (Al_T); this resonance becomes more prominent upon calcination at 773 K (Fig. 4C). These spectra exhibit no evidence of a resonance at δ 30 typical of the dehydroxylation of some aluminosilicates, which has been assigned to five-coordinate aluminium.[23] Between 773 and 1073 K, the Al_T/Al_O ratio is similar to that in γ-alumina (30–32%)[23] and although this phase was not identified by XRD, it might be present in MgO microdomains and lead to the broadened reflections in Fig. 1C. It is also worth noting that the dehydroxylation of aluminium takes place similarly as for pure gibbsite in air; alternative alumina phases such as those of cubic structure (γ-, δ- and θ-alumina) and hexagonal phases (χ- and κ-alumina) are also possible.[24] The spectrum for HT-Mg/Al calcined at 1073 K exhibits a second signal at δ *ca.* 69 (Fig. 4D) that is consistent with the chemical shift for $MgAl_2O_4$, even though no such phase is observed by XRD (Fig. 1D). Raising the calcination temperature to 1273 K increases this signal at δ 69 (Fig. 4E), consistent with the XRD results, which reveals the presence of a spinel phase.

Subsequently, solid HT-Mg/Ga was studied by ^{71}Ga MAS NMR spectroscopy. Fig. 5 shows the spectra for the solid and its calcination products. As can be seen from Fig. 5A and B, the ^{71}Ga spectra for this solid and its calcination product at 473 K both exhibit a single signal with a chemical shift in the range δ −17 and −19 that can be assigned to octahedrally coordinated gallium (Ga_O) and is consistent with previous results of our Group.[25] Calcination of this LDH at 773 K or higher temperatures introduces significant spectral changes (Fig. 5C–E); in contrast to the aluminium solids, in these gallium solids the metal is largely tetrahedrally coordinated (Ga_T, δ 58–60). Also, the Ga_O signal undergoes a downfield shift during the transformation of the LDH into Ga_2O_3 and MgO.[25] The solid calcined at 1273 K (Fig. 5E), from which, based on the XRD spectrum, the spinel is formed, exhibits an ill-defined Ga_O signal; its presence, however, can be inferred from the slope change in the spinning side band.

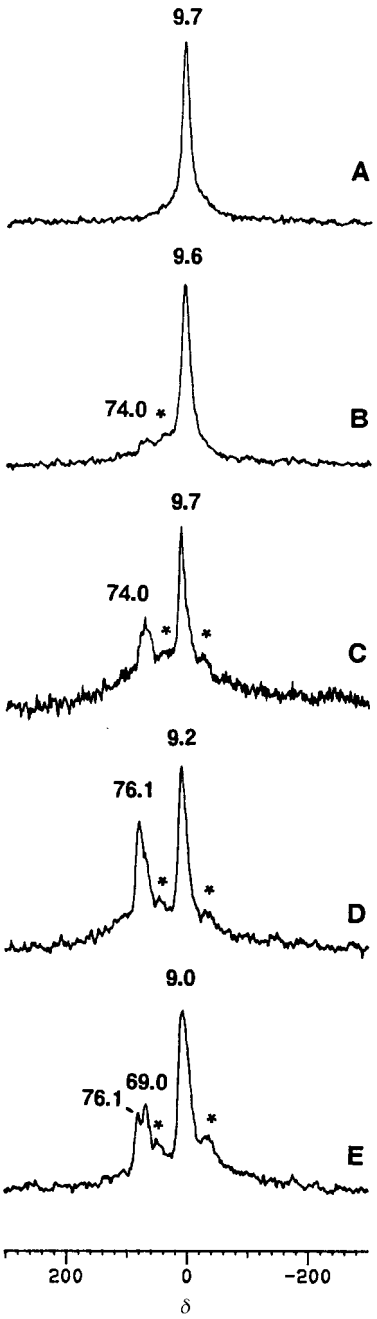

Fig. 4 ^{27}Al MAS NMR spectra for HT-Mg/Al (A) and its products of calcination at 473 K (B), 773 K (C), 1073 K (D) and 1273 K (E). *Denotes spinning side bands.

FTIR and DRIFT spectra

Fig. 6 and 7 show the FTIR and DRIFT spectra for the studied solids. FTIR spectra for HT-Mg/Al, HT-Mg/Ga and their calcination products at 473 K (Fig. 6A, B and 7A and B) exhibit strong bands between 3800 and 2700 cm^{-1} that comprises the twisting vibrations of physisorbed water,[26] vibrations of structural OH^- groups,[27] characteristic valency vibrations of OH···OH, and/or characteristic stretching vibrations of Mg^{2+}–OH^- in hydroxycarbonates.[26–29] The band corresponding to the vibration mode δ_{HOH} appears at 1647–1644 cm^{-1}. Carbonate ion in a symmetric environment exhibits three absorption bands close to those for the free anion (*viz.* ν_4 = 680 cm^{-1}, ν_2 = 880 cm^{-1} and ν_3 = 1415 cm^{-1}). Band ν_3 is clearly observed in the region 1381–1373 cm^{-1} in the four spectra, as

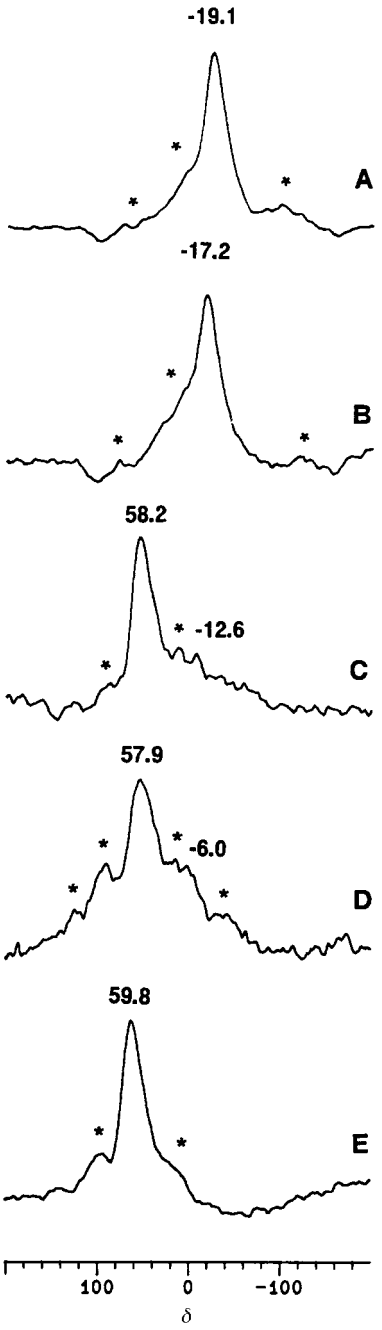

Fig. 5 ^{71}Ga MAS NMR spectra for HT-Mg/Ga (A) and its products of calcination at 473 K (B), 773 K (C), 1073 K (D) and 1273 K (E). *Denotes spinning side bands.

is ν_2 (873–874 cm^{-1}). On the other hand, the ν_4 band is only observed in the spectrum for the Mg/Al sample owing to inadequate resolution of the other three spectra. The presence of a shoulder at *ca.* 1400 cm^{-1} can be ascribed to a decreased carbonate symmetry[30] that activates the vibrational mode ν_1; this mode, which is inactive in wholly symmetric carbonate, appears as a shoulder at 1505–1535 cm^{-1} in the spectra.[31] Whilst the band at 1381–1373 cm^{-1} could correspond to ν_3 for nitrate ion; this is ruled out since nitrate ion was found to be absent following its exchange with carbonate.

Fig. 6C and 7C show DRIFT spectra for the LDHs calcined at 773 K. As can be seen, they are markedly different from the previous spectra. The spectra show prominent bands at 450–650 cm^{-1} corresponding to characteristic vibrations of the oxides (MgO, Al_2O_3, Ga_2O_3).[32,33] The spectra also include a broad band at 1400 cm^{-1} typical of O–C–O vibrations for adsorbed (non-interlayer) carbonate on the surface of the mixed

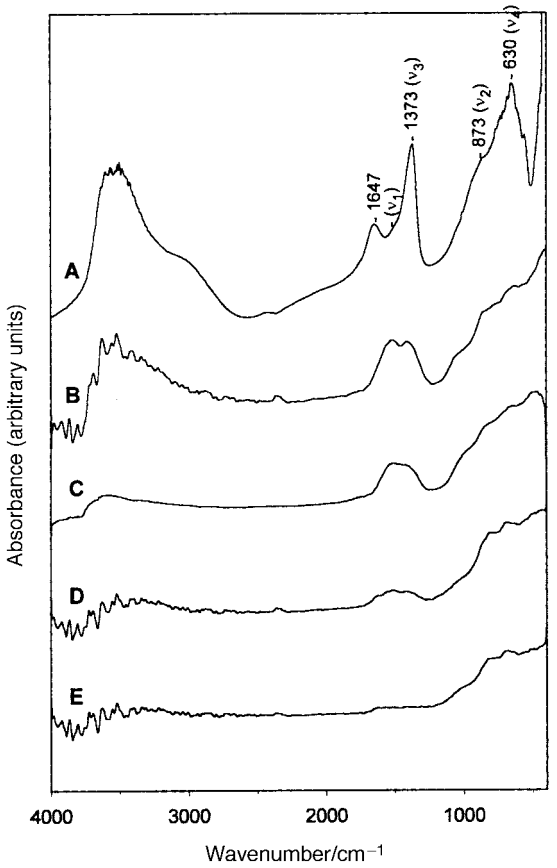

Fig. 6 IR spectra for solid HT-Mg/Al (A) and its product of calcination at 473 K (B) and DRIFT spectra for products of calcination of solid HT-Mg/Al at 773 K (C), 1073 K (D) and 1273 (E).

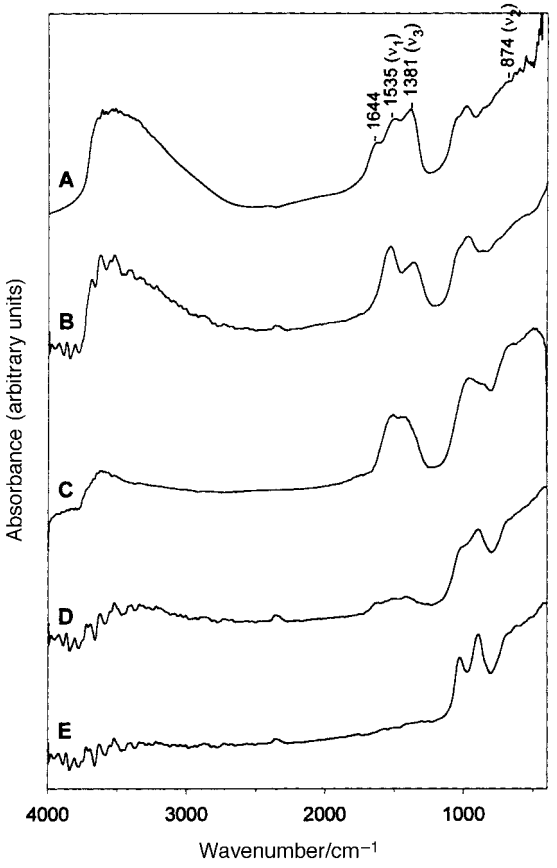

Fig. 7 IR spectra for solid HT-Mg/Ga (A) and its product of calcination at 473 K (B) and DRIFT spectra for products of calcination of solid HT-Mg/Ga at 773 K (C), 1073 K (D) and 1273 (E).

Table 1 Specific surface areas values for LDHs and their calcination products

T_{calc}/K	S_{BET} (HT-Mg/Al)[b]	S_{BET} (HT-Mg/Ga)[b]
R.T.[a]	56.2	51.7
473	58.9	61.5
773	143.5	116.9
1073	109.9	106.6
1273	75.0	48.0

[a]Room temperature. [b]Units $m^2\ g^{-1}$.

oxides formed upon calcination,[33,34] together with carbonate and water reversibly adsorbed on the oxide surfaces.[34–37] When the carbonate is forming particles or part of some other mixed structure (*e.g.* residual carbonate remaining after the synthesis of a magnesium orthophosphate), it occurs at a slightly higher frequency than interlayer carbonate,[37–39] *viz.* 1432 cm^{-1}. Finally, a further weak band is observed in the region 3800–3100 cm^{-1} arising from $OH\cdots OH_2$ and $H_2O\cdots OH_2$ groups.[27,29] Based on these results, loss of water and CO_2 from these solids is apparent.

After calcination of LDHs at 1073 and 1273 K, significant changes in the DRIFT spectra of the solids were observed (Fig. 6D, E and 7D and E). Several bands are observed in the range 400–1100 cm^{-1} which correspond to vibration bands of MgO,[32,33] Al_2O_3 and Ga_2O_3[32,40] and the spinel phases.[41]

BET results

Table 1 lists the specific surface areas for the LDHs and their calcination products. As can be seen, the areas increase with increasing calcination temperature up to 773 K, through removal of water molecules of carbon dioxide, which increases the porosity in the solids. As the calcination temperature is further increased, the specific surface area decreases to a minimum at 1273 K as a result of sintering and the formation of spinel phases. This is consistent with the XRD patterns for the solids calcined at this temperature, which exhibit narrow peaks suggestive of increased crystallinity.

Conclusions

Based on the results obtained in this work, replacement of aluminium by gallium in a layered double hydroxide introduces no substantial structural changes. The increased ionic radius of Ga^{3+} relative to Al^{3+} results in an increased interlayer spacing. Calcination of these solids at temperatures below 1073 K gives a mixture of magnesium and aluminium or gallium oxides. Above 1073 K, however, calcination yields crystalline periclase MgO phases and the aluminium or gallium spinel. As shown by MAS NMR spectra, like Ga^{3+}, Al^{3+} occupies mostly octahedral positions in the LDH structure and both octahedral and tetrahedral positions in the solids calcined above 773 K.

Acknowledgements

We wish to express our gratitude to Spain's Dirección General de Enseñanza Superior e Investigación del Ministerio de Educación y Cultura (Project PB97–0446) and the Consejería de Educación y Ciencia of the Junta de Andalucia for funding this work. The Nuclear Magnetic Resonance Service of the University of Córdoba is also gratefully acknowledged.

References

1 F. Cavani, F. Trifirò and A. Vaccari, *Catal. Today*, 1991, **11**, 173.
2 A. Corma, V. Fornés and F. Rey, *J. Catal.*, 1994, **148**, 205.
3 M. J. Climent, A. Corma, S. Iborra and J. Primo, *J. Catal.*, 1994, **151**, 215.
4 P. Courty and G. Marcilly, *Stud. Surf. Sci. Catal.*, 1983, **16**, 485.
5 F. Medina, D. Tichit, B. Coq, A. Vaccari and N. T. Dung, *J. Catal.*, 1997, **167**, 142.
6 M. Quian and H. C. Zeng, *J. Mater. Chem.*, 1997, **7**, 493.
7 G. Centi, A. Galli, B. Montanari, S. Perathoner and A. Vaccari, *Catal. Today*, 1997, **35**, 117.
8 M. A. Aramendia, V. Borau, C. Jiménez, J. M. Marinas and J. R. Ruiz, *Solid State NMR*, 1997, **8**, 251.
9 M. A. Aramendía, V. Borau, C. Jiménez, J. M. Marinas, F. J. Romero and J. R. Ruiz, *J. Solid State Chem.*, 1998, **135**, 96.
10 M. A. Aramendía, V. Borau, C. Jiménez, J. M. Marinas, F. J. Romero and J. R. Ruiz, *J. Colloid Interface Sci.*, 1998, **202**, 456.
11 M. A. Aramendía, Y. Avilés, V. Borau, C. Jiménez, J. M. Marinas, A. Moreno and J. R. Ruiz, *React. Kinet. Catal. Lett.*, 1998, **65**, 207.
12 V. R. Choudhary, A. K. Kinage, C. Sivadinarayana, P. Devadas, S. D. Sansare and M. Guisnet, *J. Catal.*, 1996, **158**, 34.
13 C.-F. Cheng, H. He, W. Zhou, J. Klinowski, J. A. Sousa Goncalves and L. F. Gladen, *J. Phys. Chem.*, 1996, **100**, 390.
14 K. J. Chao, S. P. Sehn, L.-H. Lin, M. J. Genet and J. H. Feng, *Zeolites*, 1997, **18**, 18.
15 S. Brunauer, P. H. Emmet and E. J. Teller, *J. Am. Chem. Soc.*, 1951, **60**, 73.
16 J. W. Akitt, *Annu. Rep. Spectrosc. A*, 1972, **9**, 465.
17 W. T. Reichle, S. Y. Kang and D. S. Everhardt, *J. Catal.*, 1986, **101**, 352.
18 A. De Roy, C. Forano, K. El Malki and J.-P. Besse, in *Synthesis of Microporous Materials*, ed. M. L. Occelli and H. E. Robson, Van Nostrand Reinhold, New York, 1992, vol. 2, ch. 7.
19 E. C. Kruissink, L. L. Van Reijen and J. R. H. Ross, *J. Chem. Soc., Faraday Trans. 1*, 1981, **77**, 649.
20 F. Medina, R. Dutartre, D. Tichit, B. Coq, N. T. Dung, P. Salagre and J. E. Sueiras, *J. Mol. Catal. A: Chem.*, 1997, **119**, 201.
21 M. A. Ulibarri, F. M. Labajos, V. Rives, R. Trujillano, W. Kagunya and W. Jones, *Inorg. Chem.*, 1994, **33**, 2592.
22 O. Clause, M. Gazzano, F. Trifiro, A. Vaccari and L. Zatorski, *Appl. Catal.*, 1991, **73**, 217.
23 R. H. Meinhold, R. C. T. Slade and R. H. Newman, *Appl. Magn. Reson.*, 1992, **45**, 263.
24 R. C. T. Slade, J. C. Southern and I. M. Thompson, *J. Mater. Chem.*, 1991, **1**, 563.
25 M. A. Aramendía, V. Borau, C. Jiménez, J. M. Marinas, F. J. Romero and J. R. Ruiz, *J. Solid State Chem.*, 1997, **131**, 78.
26 G. Allegra and G. Ronca, *Acta Crystallogr., Sect. A*, 1978, **34**, 1006.
27 D. Roy, R. Roy and E. Osborn, *Am. J. Sci.*, 1953, **251**, 337.
28 F. Munpton, H. Jaffe and C. Thompson, *Am. Miner.*, 1965, **50**, 1893.
29 R. Allmann, *Chimia*, 1970, **24**, 99.
30 D. L. Bish, *Program and Abstracts, 6th International Clay Conference*, Oxford, 1978.
31 M. J. Hernández-Moreno, M. A. Ulibarri, J. L Rendon and C. J. Serna, *Phys. Chem. Miner.*, 1985, **12**, 34.
32 L. Mirkin, *Rentgenostructurnii Analiz-Inducirovanic Poroshkovih Rentgenogramm*, Nakua, Moskow, 1981.
33 H. Miyata, W. Wakamiya and I. Kibokawa, *J. Catal.*, 1974, **34**, 117.
34 J. Lercher, C. Colombier, H. Vinec and H. Noller, in *Catalysis by Acids and Bases*, ed. B. Imelik, C. Maccache, G. Cardurier, Y. Ben Taarit and J. C. Vedrine, Elsevier, Amsterdam, 1985, p. 25.
35 P. Tarte, *Proceedings of the International Conference on Physics of Non-Crystalline Solids*, London, 1965, p. 549.
36 Y. Takita and J. Lunsford, *J. Phys. Chem.*, 1979, **83**, 683.
37 M. A. Aramendía, V. Borau, C. Jiménez, J. M. Marinas, F. J. Romero, J. Navio and J. Barrios, *J. Catal.*, 1995, **157**, 97.
38 K. Nakamoto, *Infrared and Raman Spectra of Inorganic Compounds*, Wiley, New York, 4th edn., 1986, p. 139.
39 K. J. D. Mackenzie, R. H. Meinhold, B. L. Sheriff and Z. Xu, *J. Mater. Chem.*, 1993, **3**, 1263.
40 J. Rabo, *Zeolite Chemistry and Catalysis*, ACS Monograph, Washington DC, 1976, part 1.
41 H. Imai, T. Takagawa and N. Kamide, *J. Catal.*, 1987, **106**, 394.

Paper 9/00535H